ISSN 0915-633X

NATIONAL INSTITUTE FOR FUSION SCIENCE

Intermittent Energy Bursts and Recurrent Topological Change of a Twisting Magnetic Flux Tube

H. Amo, T. Sato and A. Kageyama

(Received - Aug. 31, 1994)

NIFS-309 Sep.1994

RESEARCH REPORT
NIFS Series

NAGOYA, JAPAN

Intermittent Energy Bursts and Recurrent Topological Change of a Twisting Magnetic Flux Tube

Hiroyoshi Amo[1], Tetsuya Sato[1,2], and Akira Kageyama[2]

1. *Department of Fusion Science, The Graduate University for Advanced Studies, Nagoya 464-01, Japan*

2. *Theory and Computer Simulation Center, National Institute for Fusion Science, Nagoya 464-01, Japan*

When continuously twisted, a magnetic flux tube suffers a large kink distortion in the middle part of the tube, like a knot-of-tension instability of a bundle of twisted rubber strings, and reconnection is triggered starting with the twisted field lines and quickly proceeding to the untwisted field lines at the twist-untwist boundary, whereby a giant burst-like energy release takes place. Subsequently, bursts occur intermittently and reconnection advances deeper into the untwisted region. Then, a companion pair of the linked twist-untwist flux tubes reconnect with each other to return to the original axisymmetric tube. The process is thus repeatable.

Keywords: twisting magnetic flux-tube, knot-of-tension instability, driven magnetic reconnection, topological change, intermittent bursts, recurrence, self-organization

There are many phenomena in nature that manifest energy release in an off-and-on, or intermittent fashion, such as a geyser and a shishiodoshi (a bamboo-made contrivance in Japanese garden). The intermittent burst-like energy release can occur in an open system with a steady energy flow, if the energy conversion process is nonlinear.

Magnetic reconnection is believed to be an important, fundamental process that causes a burst-like energy release. Magnetospheric substorms and solar flares are typical examples which are considered to be caused by magnetic reconnection. Particularly, the driven reconnection process is the most viable process that effectively and swiftly converts the magnetic energy into the kinetic and thermal energies [1]. Magnetic field lines are easily deformed in accordance with a plasma motion in a collisionless plasma. At a stagnation or a converging point (or line) of the plasma flow it often happens that field lines with anti-parallel components approach to one another and an electric current is locally enhanced. Magnetic reconnection is then forced to take place there subject to either a classical resistivity [1] or a collisionless process [2]. This forced reconnection is called "driven" magnetic reconnection.

The photospheric convection is believed to be a primary energy source of a variety of plasma phenomena, e.g. the solar dynamo and the coronal heating. It is conjectured, therefore, that the photospheric motion also can be a primary cause of solar flares. Several authors have attempted to demonstrate the energy conversion process subject to a shear or rotating motion of the footpoint of a magnetic flux tube [3-5].

From the childhood reminiscence, one may recollect that when screwing by finger a propeller of a model airplane which is connected to a bundle of rubber strings, the twisted strings suffer a knot-of-tension instability. Knots are created one by one as one keeps on screwing the propeller. The creation of a structure lowers the energy of tension. In this sense, the knot-of-tension instability is an energy relaxation process.

From this analogy we may expect that a repeated, stepwise energy relaxation must take place when a magnetic flux tube is kept on twisting. In the case of the magnetic flux, however, it can happen that magnetic field lines are reconnected and suffer a topological change, which does not happen for the rubber strings except for a sudden break which never happens for the field lines. In the present paper we aim at elucidation of the energy relaxation and topology change processes of a twisting magnetic flux tube.

We employ a methodology of a magnetohydrodynamic simulation for a rectangular cylinder model surrounded by a conducting wall in which straight axial field lines are uniformly embedded. Cartesian coordinates (x, y, z) are adopted where the axial boundaries are placed at $z = 0$ and $z = L$ and the conducting side boundaries are placed at $x = \pm 1/2L$ and $y = \pm 1/2L$. At the axial boundaries we impose a circular motion to twist the axial magnetic field.

The axial boundary conditions for the magnetic field $\boldsymbol{B}$ and the convection flow $\boldsymbol{V}$ are specified as follows:

(1) A prescribed circular motion is applied at $z = 0$ and $z = L$ so as to twist continuously and steadily a magnetic flux tube in a circular region of the radius of $0.15L$ centered at the central axis ($x = 0$ and $y = 0$). The twist profile is described by a cubic equation of a distance r from the central axis which vanishes at the center ($x = 0$ and $y = 0$) and at the radius of $0.15L$, and is maximized at the radius of $0.1L$. The axial flow component is assumed to be zero at $z = 0$ and $z = L$ so that no material transport is allowed through the axial boundaries. (2) The line-tying condition is imposed on the magnetic field at the axial boundaries, namely, $\partial \boldsymbol{B}/\partial t = \nabla \times (\boldsymbol{V} \times \boldsymbol{B})$ is solved at $z = 0$ and L. Therefore, B_z is constant, and B_x and B_y are determined by solving the induction equation.

The plasma density is assumed to be uniform and constant ρ_0, and the thermal energy converted from the magnetic and flow energies is supposed to be immediately released outside by radiation. The resistivity and viscosity, η and μ, are assumed to be uniform and constant. All the physical quantities are normalized by the initial axial magnetic field intensity B_0,the constant density ρ_0 and the axial system length L. For example, the energy is normalized by $B_0^2/2\mu_0$ (μ_0 is the permeability), the velocity by $V_A = B_0/\sqrt{2\mu_0\rho_0}$, the time by $\tau_A = L/V_A$. The normalized resistivity, $\eta\tau_A/L^2$, is taken to be 10^{-4} and the normalized viscosity $\nu\tau_A/L^2$ to be 10^{-3}.

Since no spatial mode grows unless no spatial disturbance exists in the system, we initially give a random noise with a negligibly small amplitude upon the initial uniform configuration. Then, we start twisting the magnetic field. The magnitude of the maximum speed V_0 is given as $V_0 = 0.1V_A$.

The twisted signal propagates axially from both ends (boundaries) as an Alfven wave and bounces at each end. A half-bounce period of the signal is one Alfven transit time, $1\tau_A$. An Alfven wave carries an axial (field-aligned) current, whereby a magnetic field line is helically twisted. Since a constant twisting force (electric field) is continuously supplied at the axial boundaries, the energy supplier acts as a voltage generator. Should no energy release happen, therefore, the current would increase almost indefinitely and hence the magnetic field would be indefinitely wound up because of a tiny resistivity. This anticipates that an energy releasing process must happen eventually.

The time evolution of the volume integrated rate of conversion of the magnetic energy to the kinetic energy (work done by the Ampere force) is shown by the dashed line of Fig. 1. One finds that at around $t = 13\tau_A$ the power conversion rate exhibits a burst-like increase. Furthermore, the burst is not a single-shot but repeats quasi-periodically with intervals of $t = 5 - 7\tau_A$. The burst lasts only $1 \sim 2\tau_A$. In order to see the energy conversion process the time evolution of the total Poynting flux through the axial boundaries is simultaneously plotted by the solid line in Fig. 1.

It should be noted that the most drastic energy release takes place in association with the first burst. The energy releases associated with the second ($t \simeq 18\tau_A$) and third ($t \simeq 26\tau_A$) bursts are not so drastic as the first one. However, the energy release associated with the fourth ($t \simeq 30\tau_A$) burst becomes again drastic and this is rather similar to the first one. The reason will become clear later on.

We shall now turn our attention to the evolution of the magnetic field configuration. To see the topological change in detail, we pick up eight representative field lines which originate from equally-spaced eight points located on a central circle with radius of $r = 0.01L$ and exhibit a stereoscopic view of these field lines. In the first place we illustrate in Fig. 2 the time sequential plots of the eight field lines projected on the $x - y$ plane (upper panels) and on the $x - z$ plane (lower panels). As one sees in Fig. 2(a), the uniformly twisted flux tube suffers a large kink distortion, particularly, in the middle part of the tube, just like a knot-of-tension instability of a bundle of screwed rubber strings ($t = 12.5\tau_A$). The distortion is drastically accelerated in a very short period ($t = 12.8\tau_A$ and $13.1\tau_A$). On looking at the upper panels, one notices a very important fact that while at $t = 12.5\tau_A$ the eight lines starting from the eight points on a circle at the boundary of $z = 0$ are terminated on the same circle at the boundary of $z = L$, the terminating points start deviating from the original circle as time elapses (see, $t = 12.8\tau_A$ and $13.1\tau_A$). This deviation is nothing but the indication of the fact that the original field lines starting at $z = 0$ are reconnected with other field lines which originate from the terminating points on the $z = L$ plane. On comparing the side views of $t = 12.8\tau_A$ and $t = 13.1\tau_A$ with keeping this fact in mind, one notices an important difference, namely, at $t = 13.1\tau_A$ the twisted lines in the first half part of the tube ($z = 0 \sim 1/2L$) remain almost unchanged but the lines in the last half part ($z = 1/2L \sim L$) manifest a drastic change. This confirms that the reconnection process must have happened around $z = 0.5L$ and $r = 0.15L$ (border between twisted and untwisted regions).

Secondly, we shall observe the topological change of the magnetic field in the time range of $t = 14.0\tau_A \sim 25.0\tau_A$ during which the second burst takes place. By comparing the last panel of Fig. 2(a) ($t = 13.1\tau_A$) and the first one of Fig. 2(b) ($t = 14.0\tau_A$), one readily finds that the highly distorted reconnected structure at $t = 13.1\tau_A$ has relaxed to a rather uniformly twisted structure at $t = 14.0\tau_A$. An important feature is that during the first burst the distorted field lines accelerate reconnection at around $z = 1/2$ with neighboring distorted field lines until they reconnect with the untwisted field lines lying at the border between the twisted region and the untwisted region, namely, $r = 0.15L$ ($t = 14.0\tau_A$). At this time the first energy relaxation process ceases.

As the twisting progresses and an excess free magnetic energy is deposited further, another kink instability arises as is seen in the middle panel of Fig. 2(b) ($t = 17.0\tau_A$). In accordance with the progress of the instability, the distorted field lines advance reconnection with the more distant untwisted field lines as is clearly observed in the top view of Fig.2(b).

Figure 2(c) illustrates the topological evolution during the third burst. During this burst the field lines that originate from $z = 0$ and have reconnected with the distant outer field lines anchoring at $z = L$ are deformed so as to make reconnection with the original companion field lines that originate from $z = L$ and have reconnected with the distant outer field lines anchoring at $z = 0$. Consequently, the system returns to a more or less original configuration ($t = 26.0\tau_A$).

From these sequential events we can conclude that when a flux tube is continuously twisted, a knot-of-tension instability, or a localized kink instability, arises and reconnection progresses among the distorted field lines until the twisted field lines execute reconnection with the untwisted field lines. During this burst event the twisted magnetic energy is largely released, mostly, to the thermal energy. As the twisting continues further, another instability arises and reconnection advances to a more distant outer region. Then, the third instability stimulates reconnection with the companion field lines whereby the magnetic field configuration returns to the original axisymmetric one. The energy releases associated with the second and third instabilities are not so drastic as the first one.

The above fact that a twisting flux tube returns to the original state motivates us to conclude that as a bundle of magnetic field lines is kept on twisting, an energy relaxation and magnetic topology change would occur in a recurrent fashion.

The energy buildup and abrupt drop of the Poynting flux around $t = 30\tau_A$ of Fig. 1 manifest a recurrent energy release. Figure 2(d) illustrates the topological evolution of the magnetic field lines during the fourth burst that starts from the more or less original topology ($t = 29.0\tau_A$). As is seen in this figure, a distortion, which is very similar to what is seen at $t = 12.5\tau_A$ of Fig. 2(a), appears and reconnection advances up to the boundary of the untwisted region ($t = 31.0\tau_A$).

Finally, we look into the physical process of reconnection taking place at the border between the twisted and untwisted regions. Figure 3 shows the contours of the axial current on the $x - y$ plane at $z = L/2$ at $t = 13.1\tau_A$. As is seen in Fig. 3, a thin-current sheet (current singularity) is formed just on the twist-untwist boundary. The field lines in a twisting flux tube suffer a structural instability and tend to release the extra free tension (current) energy to the surrounding space. Since the surrounding space is at rest, the tension energy is naturally concentrated, at least transiently, at the twist-untwist boundary, thus, a current-singularity is formed at the boundary. Because of this current singularity formation, reconnection takes place predominantly around the twist-untwist boundary.

This work is carried out in pursuance of our extensive program for formulating the quantitative scientific basis of the physics of the complexity in plasma. A demonstration is given that in an open magnetohydrodynamic system where a free magnetic energy is continuously supplied and a produced thermal energy (entropy) is immediately expulsed, self-organization proceeds in two cycles, a minor cycle and a grand cycle. Energy release and topology change occur in a burst-like fashion in a minor cycle. In the grand cycle, which consists of a few minor cycles, the system recovers virtually to the original state both in energy and topology and exhibits a recurrent behavior.

The authors wish to thank all other members of the Complexity Simulation Group of NIFS. This work is performed by using the Advanced Computing System for Complexity Simulation at NIFS. This work is partially supported by two Grants-in-Aid of the Ministry of Education, Science and Culture (No. 06044238 and No. 05836038) and is also conducted as a part of a cooperative research supported by the Graduate University for Advanced Studies (GUAS). One of the authors (H.A.) wishes to express his gratitude to NEC Corporation for giving him an opportunity to conduct his Ph.D study at GUAS for three years.

---

1. T. Sato and H. Hayashi, Phys. Fluids 22, 1189-1202 (1979); T. Hayashi Sato, J. Geophs. Res. 83, 217-220 (1978)
2. R. Horiuchi and T. Sato, Phys. Plasmas (in press)
3. Z. Mikic, D. C. Barnes and D. D. Schnack, Astrophy. J. 328, 830-847 (1988)
4. D. Biskamp and H. Welter, Solar Phys. 120, 49-77 (1989)
5. K. Kusano, Y. Suzuki, H. Kubo, T. Miyoshi and Nishikawa, Astrophy. J. (in press)

Figure Captions

Fig. 1 Time evolutions of the Poynting flux through two axial boundaries and the work done by the $\mathbf{J} \times \mathbf{B}$ force to accelerate the plasma.

Fig. 2 Stereoscopic view of the distortion and topological change of the twisted field lines due to a knot-of-tension instability.

(a) The knot structure grows and reconnection takes place among the highly distorted field lines ($t = 13.1\tau_A$).

(b) The distorted twisted field lines proceed reconnection with untwisted field lines from the twist-untwist boundary to a distant untwisted region during the second burst (t=17-18τ_A).

(c) During the fourth burst (t=24-26τ_A) a companion pair of the reconnected twisted-untwisted field lines reconnect with each other and return to a more or less original straight flux tube of twisted field lines.

(d) The straight flux tube of twisted field lines repeat intermittent bursts similar to what happened in Fig. 2(a) - (c).

Fig. 3 A current singularity appears at the twist-untwist boundary where reconnection is predominantly driven.

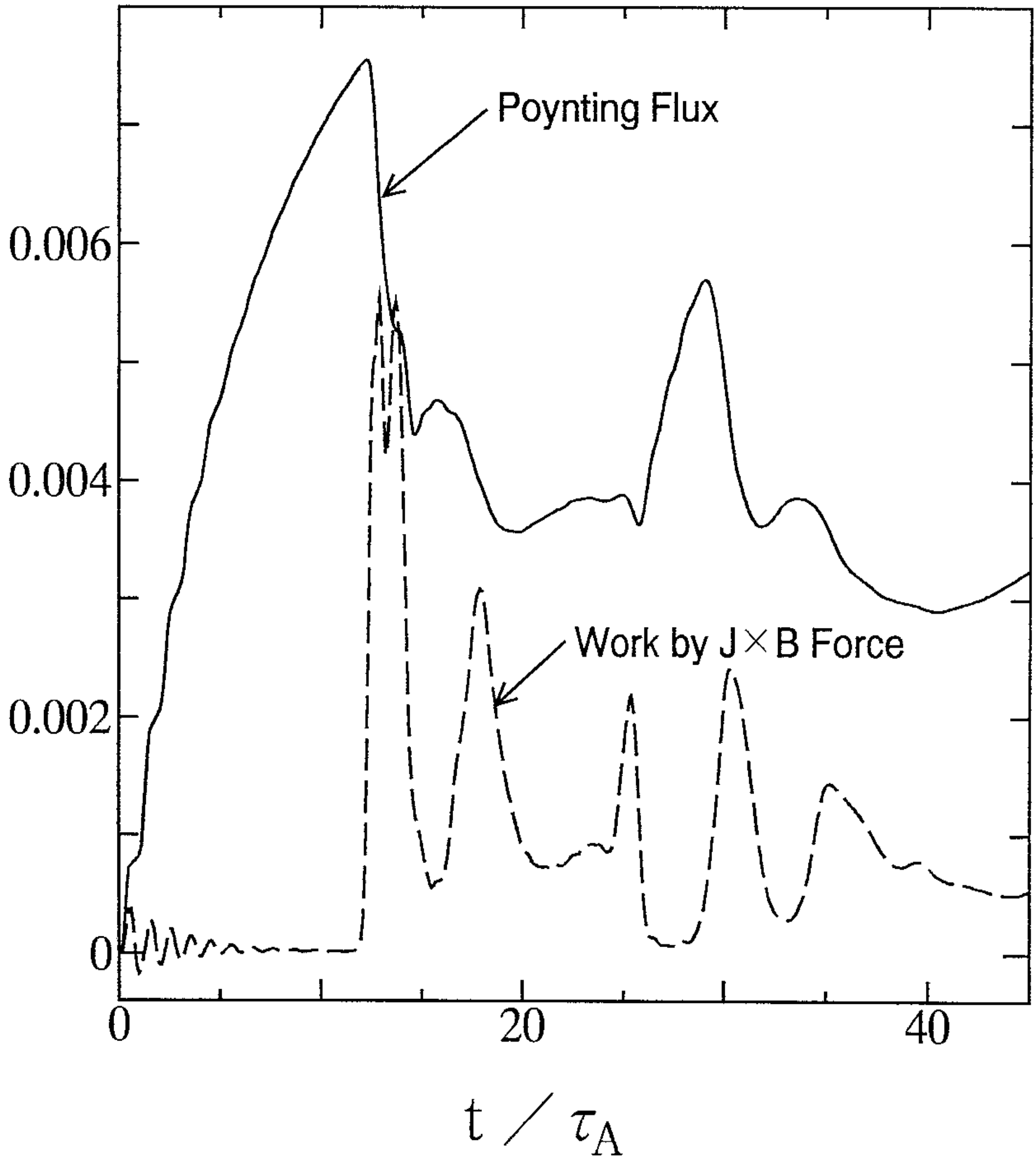

Fig. 1

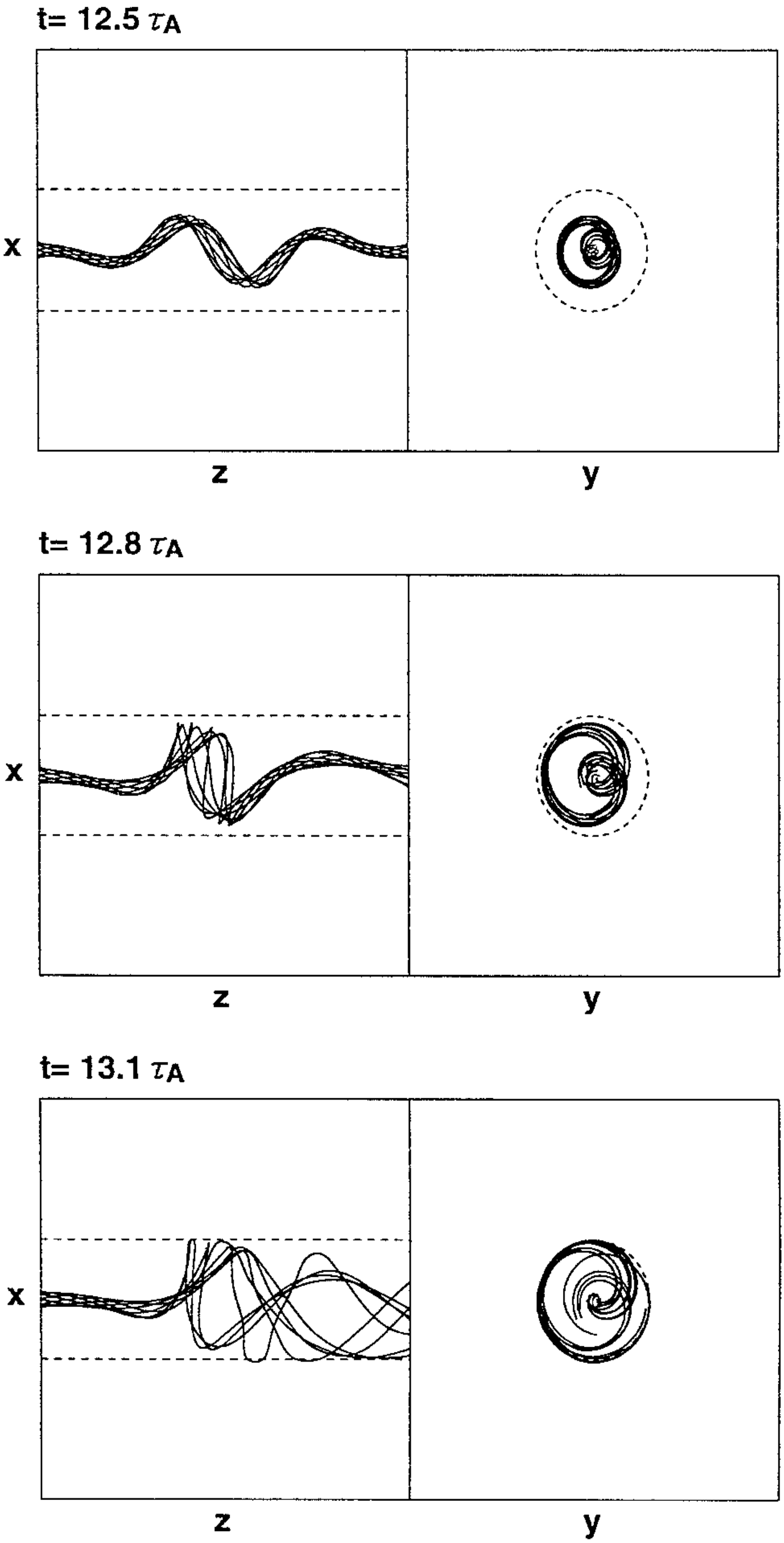
$t= 12.5\ \tau_{\mathrm{A}}$
x
z
y
$t= 12.8\ \tau_{\mathrm{A}}$
x
z
y
$t= 13.1\ \tau_{\mathrm{A}}$
x
z
y

Fig.2(a)

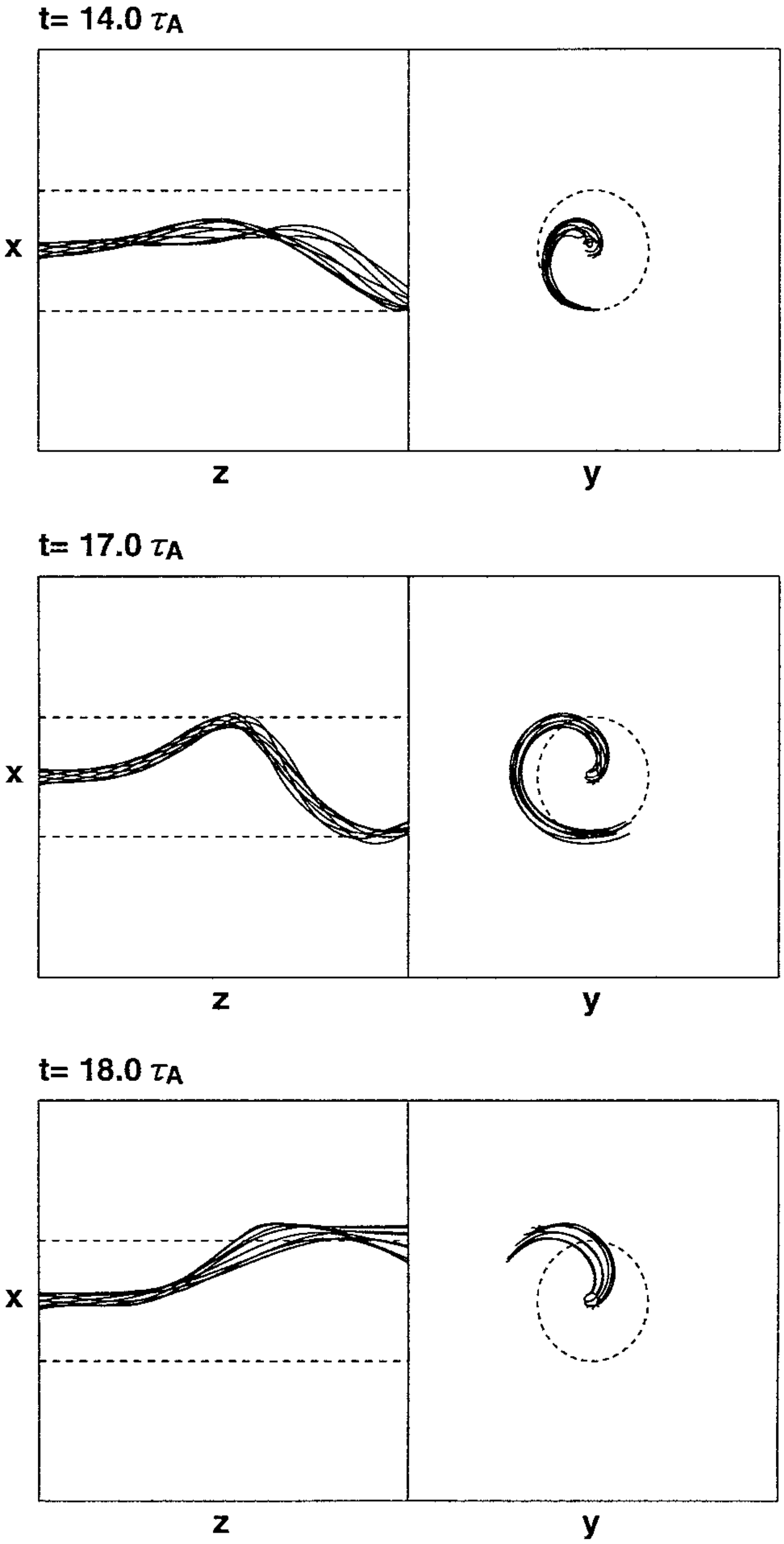

Fig.2(b)

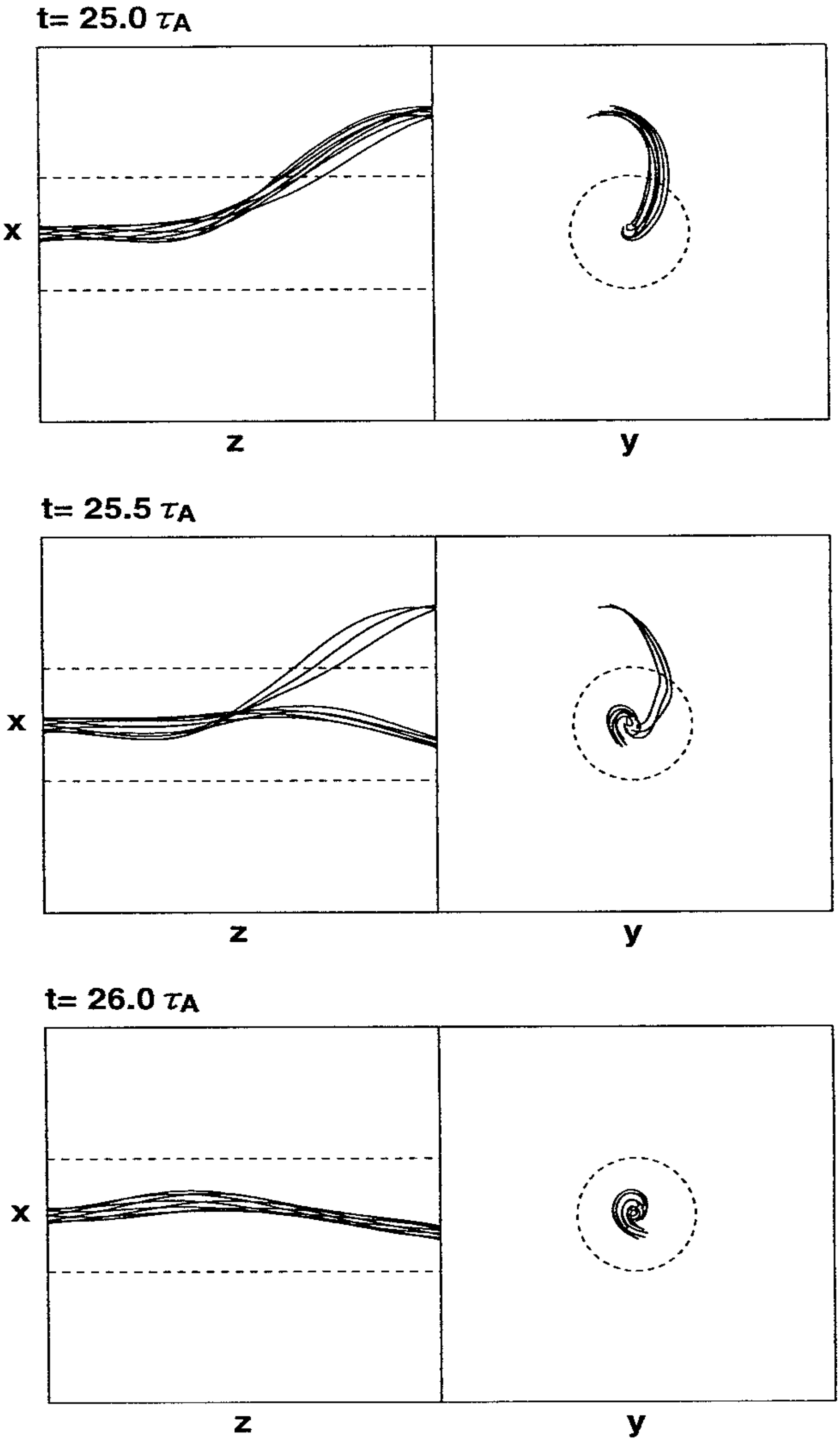

$t = 25.0\ \tau_A$

$t = 25.5\ \tau_A$

$t = 26.0\ \tau_A$

Fig.2(c)

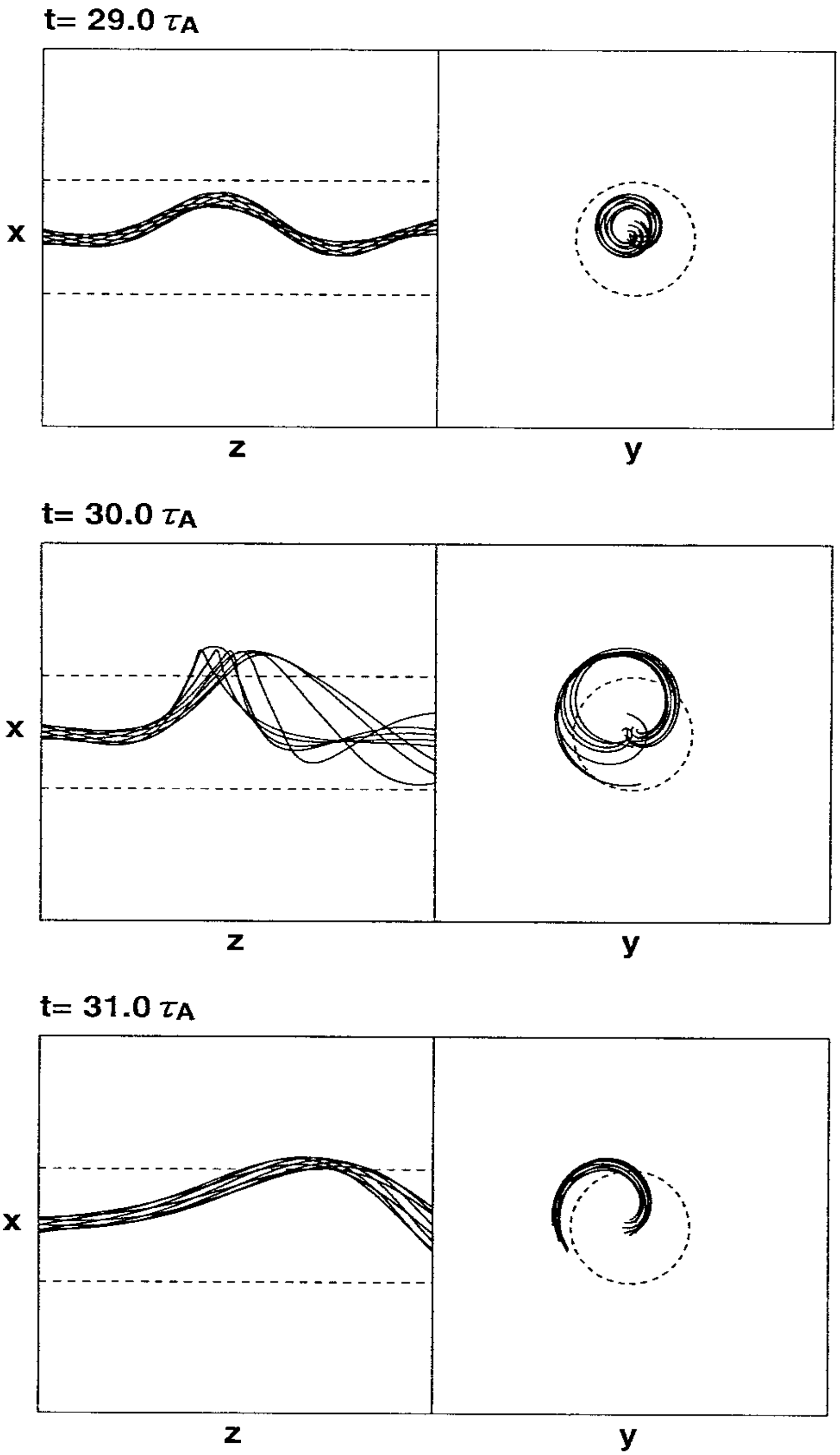

Fig.2(d)

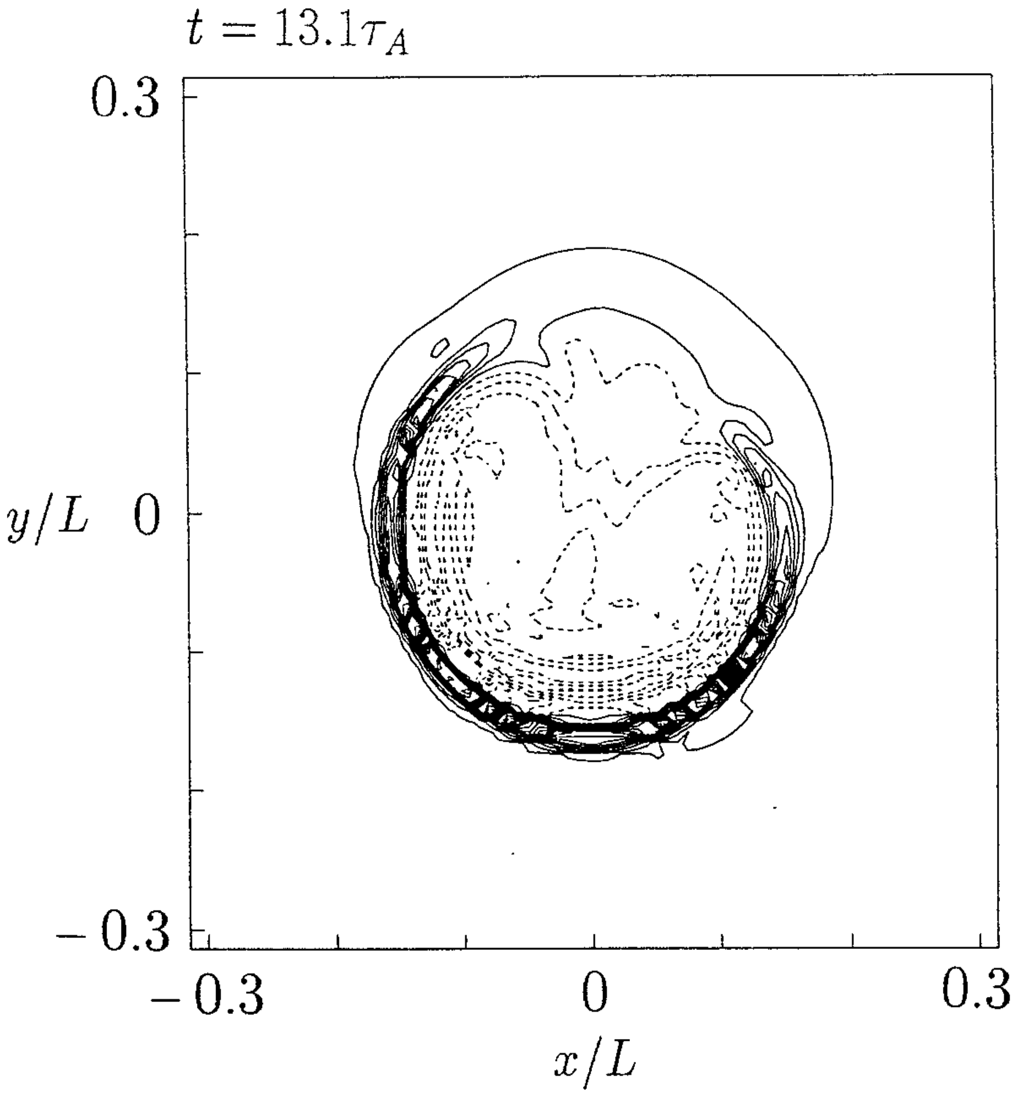

Fig. 3

Recent Issues of NIFS Series

NIFS-272	A. Fujisawa, H. Iguchi, A. Taniike, M. Sasao, Y. Hamada, *A 6MeV Heavy Ion Beam Probe for the Large Helical Device*; Feb. 1994
NIFS-273	Y. Hamada, A. Nishizawa, Y. Kawasumi, K. Narihara, K. Sato, T. Seki, K. Toi, H. Iguchi, A. Fujisawa, K. Adachi, A. Ejiri, S. Hidekuma, S. Hirokura, K. Ida, J. Koong, K. Kawahata, M. Kojima, R. Kumazawa, H. Kuramoto, R. Liang, H. Sakakita, M. Sasao, K. N. Sato, T. Tsuzuki, J. Xu, I. Yamada, T. Watari, I. Negi, *Measurement of Profiles of the Space Potential in JIPP T-IIU Tokamak Plasmas by Slow Poloidal and Fast Toroidal Sweeps of a Heavy Ion Beam*; Feb. 1994
NIFS-274	M. Tanaka, *A Mechanism of Collisionless Magnetic Reconnection*; Mar. 1994
NIFS-275	A. Fukuyama, K. Itoh, S.-I. Itoh, M. Yagi and M. Azumi, *Isotope Effect on Confinement in DT Plasmas*; Mar. 1994
NIFS-276	R.V. Reddy, K. Watanabe, T. Sato and T.H. Watanabe, *Impulsive Alfven Coupling between the Magnetosphere and Ionosphere*; Apr.1994
NIFS-277	J. Uramoto, *A Possibility of π^- Meson Production by a Low Energy Electron Bunch and Positive Ion Bunch*; Apr. 1994
NIFS-278	K. Itoh, S.-I. Itoh, A. Fukuyama, M. Yagi and M. Azumi, *Self-sustained Turbulence and L-mode Confinement in Toroidal Plasmas II*; Apr. 1994
NIFS-279	K. Yamazaki and K.Y.Watanabe, *New Modular Heliotron System Compatible with Closed Helical Divertor and Good Plasma Confinement*; Apr. 1994
NIFS-280	S. Okamura, K. Matsuoka, K. Nishimura, K. Tsumori, R. Akiyama, S. Sakakibara, H. Yamada, S. Morita, T. Morisaki,. N. Nakajima, K. Tanaka, J. Xu, K. Ida, H. Iguchi, A. Lazaros, T. Ozaki, H. Arimoto, A. Ejiri, M. Fujiwara, H. Idei. O. Kaneko, K. Kawahata, T. Kawamoto, A. Komori, S. Kubo, O. Motojima, V.D. Pustovitov, C. Takahashi, K. Toi and I. Yamada, *High-Beta Discharges with Neutral Beam Injection in CHS*; Apr. 1994
NIFS-281	K. Kamada, H. Kinoshita and H. Takahashi, *Anomalous Heat Evolution of Deuteron Implanted Al on Electron Bombardment* ; May 1994

NIFS-282 H. Takamaru, T. Sato, K. Watanabe and R. Horiuchi,
Super Ion Acoustic Double Layer; May 1994

NIFS-283 O.Mitarai and S. Sudo
Ignition Characteristics in D-T Helical Reactors; June 1994

NIFS-284 R. Horiuchi and T. Sato,
Particle Simulation Study of Driven Magnetic Reconnection in a Collisionless Plasma; June 1994

NIFS-285 K.Y. Watanabe, N. Nakajima, M. Okamoto, K. Yamazaki, Y. Nakamura, M. Wakatani,
Effect of Collisionality and Radial Electric Field on Bootstrap Current in LHD (Large Helical Device); June 1994

NIFS-286 H. Sanuki, K. Itoh, J. Todoroki, K. Ida, H. Idei, H. Iguchi and H. Yamada,
Theoretical and Experimental Studies on Electric Field and Confinement in Helical Systems; June 1994

NIFS-287 K. Itoh and S-I. Itoh,
Influence of the Wall Material on the H-mode Performance; June 1994

NIFS-288 K. Itoh, A. Fukuyama, S.-I. Itoh, M. Yagi and M. Azumi
Self-Sustained Magnetic Braiding in Toroidal Plasmas: July 1994

NIFS-289 Y. Nejoh,
Relativistic Effects on Large Amplitude Nonlinear Langmuir Waves in a Two-Fluid Plasma; July 1994

NIFS-290 N. Ohyabu, A. Komori, K. Akaishi, N. Inoue, Y. Kubota, A.I. Livshit, N. Noda, A. Sagara, H. Suzuki, T. Watanabe, O. Motojima, M. Fujiwara, A. Iiyoshi,
Innovative Divertor Concepts for LHD; July 1994

NIFS-291 H. Idei, K. Ida, H. Sanuki, S. Kubo, H. Yamada, H. Iguchi, S. Morita, S. Okamura, R. Akiyama, H. Arimoto, K. Matsuoka, K. Nishimura, K. Ohkubo, C. Takahashi, Y. Takita, K. Toi, K. Tsumori and I. Yamada,
Formation of Positive Radial Electric Field by Electron Cyclotron Heating in Compact Helical System; July 1994

NIFS-292 N. Noda, A. Sagara, H. Yamada, Y. Kubota, N. Inoue, K. Akaishi, O. Motojima, K. Iwamoto, M. Hashiba, I. Fujita, T. Hino, T. Yamashina, K. Okazaki, J. Rice, M. Yamage, H. Toyoda and H. Sugai,
Boronization Study for Application to Large Helical Device; July 1994

NIFS-293 Y. Ueda, T. Tanabe, V. Philipps, L. Könen, A. Pospieszczyk, U. Samm, B. Schweer, B. Unterberg, M. Wada, N. Hawkes and N. Noda, *Effects of Impurities Released from High Z Test Limiter on Plasma Performance in TEXTOR*; July. 1994

NIFS-294 K. Akaishi, Y. Kubota, K. Ezaki and O. Motojima,
Experimental Study on Scaling Law of Outgassing Rate with A Pumping Parameter, Aug. 1994

NIFS-295 S. Bazdenkov, T. Sato, R. Horiuchi, K. Watanabe
Magnetic Mirror Effect as a Trigger of Collisionless Magnetic Reconnection, Aug. 1994

NIFS-296 K. Itoh, M. Yagi, S.-I. Itoh, A. Fukuyama, H. Sanuki, M. Azumi
Anomalous Transport Theory for Toroidal Helical Plasmas,
Aug. 1994 (IAEA-CN-60/D-III-3)

NIFS-297 J. Yamamoto, O. Motojima, T. Mito, K. Takahata, N. Yanagi, S. Yamada, H. Chikaraishi, S. Imagawa, A. Iwamoto, H. Kaneko, A. Nishimura, S. Satoh, T. Satow, H. Tamura, S. Yamaguchi, K. Yamazaki, M. Fujiwara, A. Iiyoshi and LHD group,
New Evaluation Method of Superconductor Characteristics for Realizing the Large Helical Device; Aug. 1994 (IAEA-CN-60/F-P-3)

NIFS-298 A. Komori, N. Ohyabu, T. Watanabe, H. Suzuki, A. Sagara, N. Noda, K. Akaishi, N. Inoue, Y. Kubota, O Motojima, M. Fujiwara and A. Iiyoshi,
Local Island Divertor Concept for LHD; Aug. 1994 (IAEA-CN-60/F-P-4)

NIFS-299 K. Toi, T. Morisaki, S. Sakakibara, A. Ejiri, H. Yamada, S. Morita, K. Tanaka, N. Nakjima, S. Okamura, H. Iguchi, K. Ida, K. Tsumori, S. Ohdachi, K. Nishimura, K. Matsuoka, J. Xu, I. Yamada, T. Minami, K. Narihara, R. Akiyama, A. Ando, H. Arimoto, A. Fujisawa, M. Fujiwara, H. Idei, O. Kaneko, K. Kawahata, A. Komori, S. Kubo, R. Kumazawa, T. Ozaki, A. Sagara, C. Takahashi, Y. Takita and T. Watari
Impact of Rotational-Transform Profile Control on Plasma Confinement and Stability in CHS; Aug. 1994 (IAEA-CN-60/A6/C-P-3)

NIFS-300 H. Sugama and W. Horton,
Dynamical Model of Pressure-Gradient-Driven Turbulence and Shear Flow Generation in L-H Transition; Aug. 1994 (IAEA/CN-60/D-P-I-11)

NIFS-301 Y. Hamada, A. Nishizawa, Y. Kawasumi, K.N. Sato, H. Sakakita, R. Liang, K. Kawahata, A. Ejiri, K. Narihara, K. Sato, T. Seki, K. Toi, K. Itoh, H. Iguchi, A. Fujisawa, K. Adachi, S. Hidekuma, S. Hirokura, K. Ida, M. Kojima, J. Koog, R. Kumazawa, H. Kuramoto, T. Minami, I. Negi, S. Ohdachi, M. Sasao, T. Tsuzuki, J. Xu, I. Yamada, T. Watari,
Study of Turbulence and Plasma Potential in JIPP T-IIU Tokamak;
Aug. 1994 (IAEA/CN-60/A-2-III-5)

NIFS-302 K. Nishimura, R. Kumazawa, T. Mutoh, T. Watari, T. Seki, A. Ando, S. Masuda, F. Shinpo, S. Murakami, S. Okamura, H. Yamada, K. Matsuoka,

S. Morita, T. Ozaki, K. Ida, H. Iguchi, I. Yamada, A. Ejiri, H. Idei, S. Muto, K. Tanaka, J. Xu, R. Akiyama, H. Arimoto, M. Isobe, M. Iwase, O. Kaneko, S. Kubo, T. Kawamoto, A. Lazaros, T. Morisaki, S. Sakakibara, Y. Takita, C. Takahashi and K. Tsumori, *ICRF Heating in CHS*; Sep. 1994 (IAEA-CN-60/A-6-I-4)

NIFS-303 S. Okamura, K. Matsuoka, K. Nishimura, K. Tsumori, R. Akiyama, S. Sakakibara, H. Yamada, S. Morita, T. Morisaki, N. Nakajima, K. Tanaka, J. Xu, K. Ida, H. Iguchi, A. Lazaros, T. Ozaki, H. Arimoto, A. Ejiri, M. Fujiwara, H. Idei, A. Iiyoshi, O, Kaneko, K. Kawahata, T. Kawamoto, S. Kubo, T. Kuroda, O. Motojima, V.D. Pustovitov, A. Sagara, C. Takahashi, K. Toi and I. Yamada, *High Beta Experiments in CHS*; Sep. 1994 (IAEA-CN-60/A-2-IV-3)

NIFS-304 K. Ida, H. Idei, H. Sanuki, K. Itoh, J. Xu, S. Hidekuma, K. Kondo, A. Sahara, H. Zushi, S.-I. Itoh, A. Fukuyama, K. Adati, R. Akiyama, S. Bessho, A. Ejiri, A. Fujisawa, M. Fujiwara, Y. Hamada, S. Hirokura, H. Iguchi, O. Kaneko, K. Kawahata, Y. Kawasumi, M. Kojima, S. Kubo, H. Kuramoto, A. Lazaros, R. Liang, K. Matsuoka, T. Minami, T. Mizuuchi, T. Morisaki, S. Morita, K. Nagasaki, K. Narihara, K. Nishimura, A. Nishizawa, T. Obiki, H. Okada, S. Okamura, T. Ozaki, S. Sakakibara, H. Sakakita, A. Sagara, F. Sano, M. Sasao, K. Sato, K.N. Sato, T. Saeki, S. Sudo, C. Takahashi, K. Takaka, K. Tsumori, H.Yamada, I. Yamada, Y. Takita, T. Tuzuki, K. Toi and T. Watari, *Control of Radial Electric Field in Torus Plasma;* Sep. 1994 (IAEA-CN-60/A-2-IV-2)

NIFS-305 T. Hayashi, T. Sato, N. Nakajima, K. Ichiguchi, P. Merkel, J. Nührenberg, U. Schwenn, H. Gardner, A. Bhattacharjee and C.C.Hegna, *Behavior of Magnetic Islands in 3D MHD Equilibria of Helical Devices*; Sep. 1994 (IAEA-CN-60/D-2-II-4)

NIFS-306 S. Murakami, M. Okamoto, N. Nakajima, K.Y. Watanabe, T. Watari, T. Mutoh, R. Kumazawa and T. Seki, *Monte Carlo Simulation for ICRF Heating in Heliotron/Torsatrons*; Sep. 1994 (IAEA-CN-60/D-P-I-14)

NIFS-307 Y. Takeiri, A. Ando, O. Kaneko, Y. Oka, K. Tsumori, R. Akiyama, E. Asano, T. Kawamoto, T. Kuroda, M. Tanaka and H. Kawakami *Development of an Intense Negative Hydrogen Ion Source with a Wide-Range of External Magnetic Filter Field*; Sep. 1994

NIFS-308 T. Hayashi, T. Sato, H.J. Gardner and J.D. Meiss, *Evolution of Magnetic Islands in a Heliac*; Sep. 1994